Scientia Iranica A (2013) 20(6), 1626–1636

Sharif University of Technology
Scientia Iranica
Transactions A: Civil Engineering
www.scientiairanica.com

Mechanical properties of steel fiber-reinforced concrete slab tracks on non-ballasted foundations

M. Madhkhan[a,*], A. Entezam[b] and M.E. Torki[c]

a. *Department of Civil Engineering, Isfahan University of Technology, Isfahan, P.O. Box 8415683111, Iran.*
b. *Civil Group, Department of Engineering, Bou-Ali Sina University, Hamadan, P.O. Box 651744161, Iran.*
c. *Department of Civil Engineering, Sharif University of Technology, Tehran, P.O. Box 113658639, Iran.*

Received 30 July 2012; received in revised form 30 December 2012; accepted 20 April 2013

KEYWORDS
Slab track;
Steel fiber-reinforced concrete;
Spanning behavior;
Load-deflection curve;
(Concrete) Tensile strength.

Abstract. Mechanical properties of slab tracks on a foundation with nonlinear stiffness are accounted for. At first, the cracking stages were inspected in FEM models, and it was learned that slab tracks have one-way flexural behavior. Secondly, experimental full-scale models were made, and the accuracy of analyses was verified by comparing the FEM load-deflection curves with those of previous studies and validating the cracking and ultimate loads with those obtained from experiments. Finally, the effects of several parameters on the cracking and ultimate loads and the energy absorption of steel fiber-reinforced slab tracks were investigated by examining the real behavior of slab tracks on elastic foundations before and after cracking. Steel fibers increased the compressive and flexural strengths as well as ductility and energy absorption. The 2.5 m width was the optimal width and the fracture pattern changed at this width. Finally, based on the obtained fracture loads, design curves were plotted for AASHTO's factored loads.

© 2013 Sharif University of Technology. All rights reserved.

1. Introduction

The application of non-ballasted railways, especially in tunnels and bridges, has been extended widely because of reducing the height of railways, reducing the maintenance and total costs, increasing the service life of the railway, facilitating the higher velocity of trains, and increasing the lateral strength of the railway [1,2]. On the other hand, the use of steel fibers as reinforcement in concrete has been extensively increased since 1970 for many reasons, including considerably increasing flexibility and energy absorption, increasing mechanical and durability properties such as compressive, tensile, flexural, shear, and impact strength, as well as resistance against freeze and thaw, creep, shrinkage, cavitation, and corrosion. In particular, steel fiber-reinforced concrete has proved very efficacious under dynamic (especially impact) or abrasive loads, especially in pavements and piles [3-5]. In particular, when concrete is placed in situ with a finishing machine, using steel fiber-reinforced concrete is advisable because of having much working convenience and high casting speed.

The finite-element study of concrete slabs placed on elastic foundations has received increasing notice. Barros and Figueiras [6] studied the mechanical behavior of slabs reinforced with 40 kg/m^3 steel fibers. They performed their experiments in a way similar to those of Falkner and Teutsch [7], and observed very good agreement between the experimental load-deflection curves with the curves obtained from finite-element analyses. They also predicted the cracking behavior of slabs and estimated the effect of foundation stiffness (known as Foundation Modulus) on it. A number of parametric studies concerning the mechanical properties of slab

*. *Corresponding author. Tel.: +98 311 3913851, Fax: +98 311 3912700*
Email-addresses: madhkhan@cc.iut.ac.ir (M. Madhkhan); mohamad_torky@yahoo.com (M. Ebrahim Torki)

tracks on non-ballasted foundations were worked in the Iranian Ministry of Routes and Traffic [8]. The results expressed that the foundation modulus has the most significant effect on all parameters, including internal forces, stresses and displacements. It was also observed that the properties of the rails, e.g. the moment of inertia, do not markedly influence these parameters but lead to more homogeneous distribution of loads on the slab.

Numerous works dealing with the effects of fibers on the mechanical properties of slabs are reported in literature. The effects of length and the volumetric percentage of steel fibers on the energy absorption of concrete slabs with various compressive strengths were investigated by Khaloo and Afshari [9]. They deduced that longer fibers and higher volumetric contents of steel fibers provide more energy absorption, but the size and content of fibers do not remarkably influence the ultimate flexural capacity of the slab. The mechanical behavior of normal and high-strength steel fiber-reinforced concrete slab-column connections under gravity and lateral loads was investigated by Smadi and Bani Yasin [10]. They examined parameters, including the compressive strength of concrete, the type and volumetric percentage of steel fibers, and the moment-to-shear ratio. They obtained higher stiffness and smaller crack widths with the presence of steel fibers in both normal and high-strength concrete. However, incorporating steel fibers with high-strength concrete proved to further develop the overall deformation properties and resulted in less sudden and more gradual failure mode. The mechanical properties of hollow-cored reinforced concrete slab tracks on non-ballasted elastic foundations were investigated by Madhkhan et al. [11]. They concluded that hollow-cored slab tracks prove, mechanically, as efficient, under typical vehicular loads, as completely solid ones, even though they weigh 30 percent less.

Although numerous studies have been worked out dealing with steel fiber-reinforced concrete slabs to the best of the authors' knowledge, parametric studies on the mechanical properties of reinforced concrete slab tracks on elastic foundations are few. In the present work, at first, the cracking behavior of slab tracks is studied using FEM models, and it is seen that slab tracks have one-way flexural behavior. Since it is not convenient to make real laboratory models for slab tracks on elastic foundations, FEM models were made for this purpose. To assure the correctness of the models, the load-deflection curves obtained from FEM analyses for steel fiber-reinforced slab tracks were compared to the results obtained by Barros and Figueiras [6], and the agreement between the two results were satisfactory. Also, the cracking and ultimate loads in FEM models with zero foundation stiffness were validated with those obtained from experimental models. Finally, the real behavior of slab tracks on elastic foundations, before and after cracking, was studied by applying monotonic loads on FEM models. Finally, curves were plotted for design purposes under loads exerted according to AASHTO. The results can be used as a benchmark.

2. Material Properties

2.1. Reinforced Concrete

2.1.1. Concrete compressive stress-strain curve

To define the compressive stress-strain pattern for concrete, Eq. (1) is used [6]:

$$\sigma = \frac{E_c \varepsilon}{1 + (\varepsilon/\varepsilon_0)^2}, \tag{1}$$

where σ is the stress, ε is the strain, E_c is the concrete elasticity modulus, and ε_0 is the strain corresponding to the maximum stress, which can be obtained by using Timoshenko's formula [12]:

$$\varepsilon_0 = 2\frac{f'_c}{E_c}. \tag{2}$$

All the same, for plain concrete, f'_c was considered 50 MPa, based on the compressive tests, and ε_0 was recommended to be taken as 0.0024 mm/mm by Madhkhan [13].

2.1.2. Steel fiber-reinforced concrete

The fiber used in this research is steel fiber, whose geometric properties are depicted in Figure 1. The research work done by Barros and Figueiras [6] was

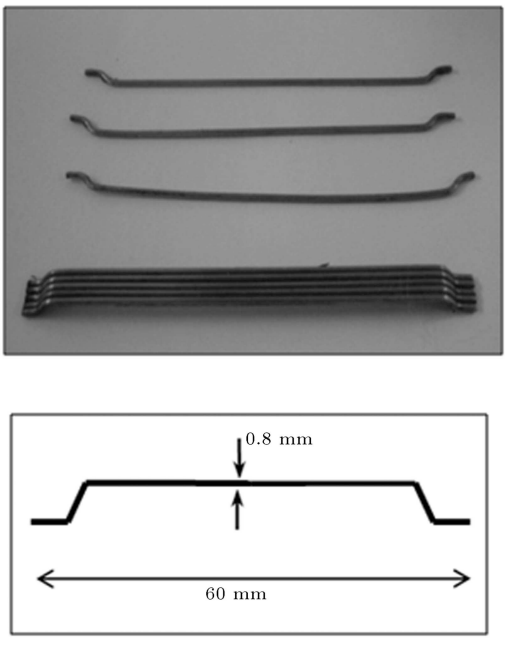

Figure 1. The shape and geometric properties of steel fibers used in the present research.

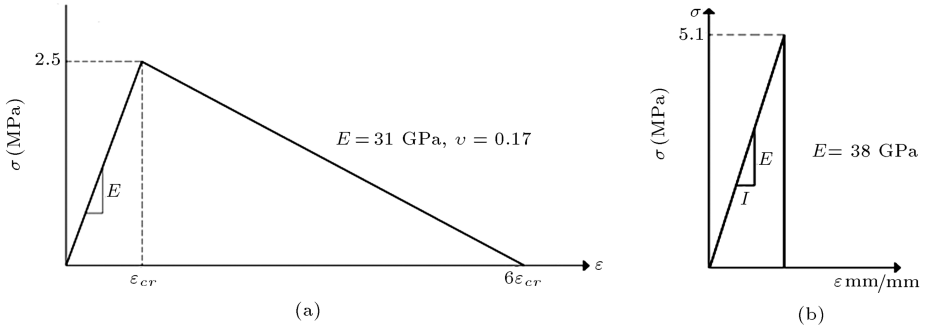

Figure 2. The tensile stress-strain model used in verification of the analyses for (a) steel fiber-reinforced concrete and (b) plain concrete.

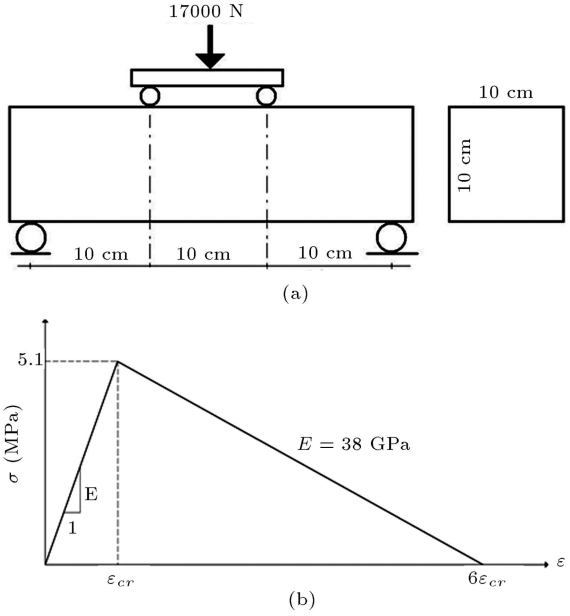

Figure 3. (a) The five-point bending test to obtain the tensile strength. (b) The tensile stress-strain model used in the main FEM analyses.

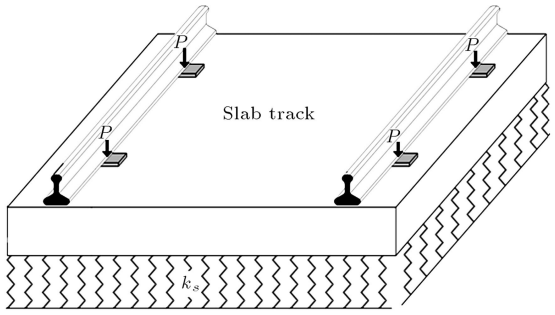

Figure 4. The schematic model of a discrete slab track system on foundation.

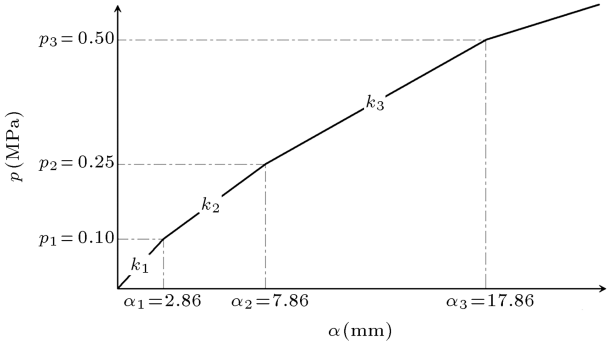

Figure 5. The total coarse and fine aggregates grading diagram.

to validate the precision of FEM results. To do so, the stress-strain pattern shown in Figure 2(a) was used, which has been simplified from a four-line diagram. In contrast to plain concrete, as shown in Figure 2(b), fiber-reinforced concrete faces softening but does not fail, whereas plain concrete is supposed to damage immediately after initial cracking. However, the main tensile stress-strain relation used in FEM analyses for fiber-reinforced concrete is shown in Figure 3(b). In this case, based on the method proposed by Vellore et al. [14], the tensile strength was calculated, based on the experimental three-point bending test on the prismatic specimen, as shown in Figure 3(a). The loading circumstance will be discussed in Section 4.2.

2.2. Slab Track Foundation

The foundation considered by Barros and Figueiras in [6] was cork. The same model was used for the foundations in this research. The schematic model of the slab on foundation is shown in Figure 4. Figure 5 shows the nonlinear behavior of the foundation underlying slabs, where p and a are the force and displacement of the foundation, respectively.

In order to have realistic load-deflection curves, RC slabs and foundations were modeled using solid and combin elements, respectively.

3. Experimental Models

As will be discussed in Section 4.1, the main objective in making experimental models is to validate FEM analyses with experimental results. To this end, 3 steel fiber-reinforced slabs with $2 \times 1.5 \times 0.215$ mdimensions were prepared. The hooked end steel fiber used had a 60 mm length, a 0.8 mm diameter, the aspect ratio of 75, and a 1000 MPa tensile strength. The volumetric

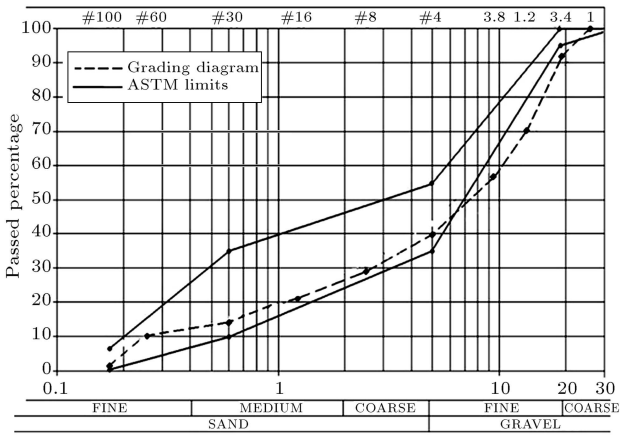

Figure 6. Mechanical behavior of the slab foundation in [6].

Table 1. Properties of the final mix design of experimental specimens (kg/m^3).

Coarse aggregates	Fine aggregates	Water	Cement	Silica fume
735	800	170	540	60

amounts of steel fiber were 40, 60, and 80 kg/m^3. The coarse aggregates, i.e. gravel, used in the mix design were crushed 50-100 mm stones, and the fine aggregates were 0-5 mm river sand with a 3.2 fineness module. The final design grading of the specimens is shown in Figure 6, which conforms well to ASTM C1018 limits [15]. Since fibers reduce fresh concrete workability to a large extent, it was vital to use ARAX SF800 superplasticizing agent, which was introduced with an amount equal to 1.5 percent of cement weight. The final mix design of the specimens is included in Table 1.

The slabs under experiment had 1.5 m widths, as shown in Figure 7. The reason is that, as followed in 5.1, slab tracks with 1.5 m width are devoid of negative moment, and thus validation of the results will be easier. Using displacement control, the slabs were put under monotonic load, according to the method put forward in [16]. The load-deflection curve for slabs (without foundation) with different fiber content is demonstrated in Figure 8. It was observed, in all experiments, that fracture takes place through a main crack in the maximum-moment zone.

4. Numerical Results

4.1. Validation with previous works

As stated earlier, the dimensions of FEM models were identical to those of full-scale experimental specimens. At first, in order to make sure that the slab foundation with the parameters defined in Section 2 is realistic, the load-deflection curve for steel fiber-reinforced concrete

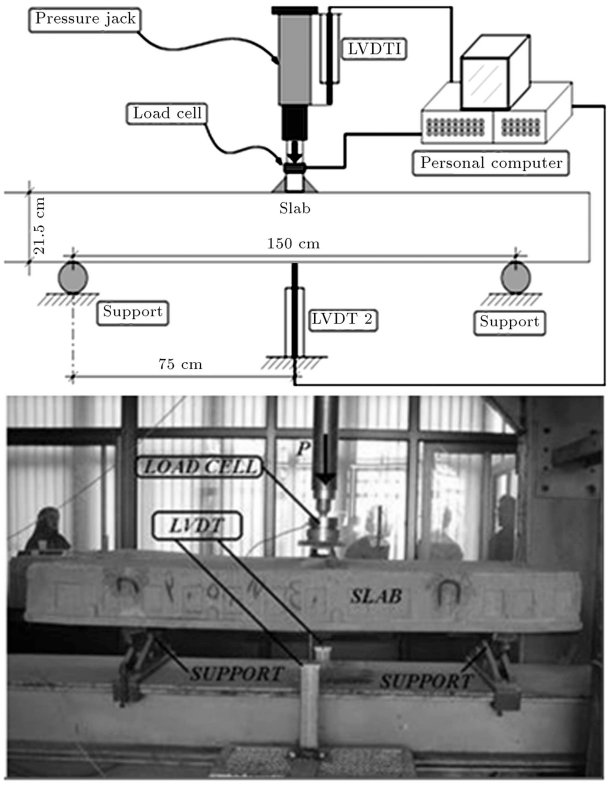

Figure 7. The setup of the bending test with centric load.

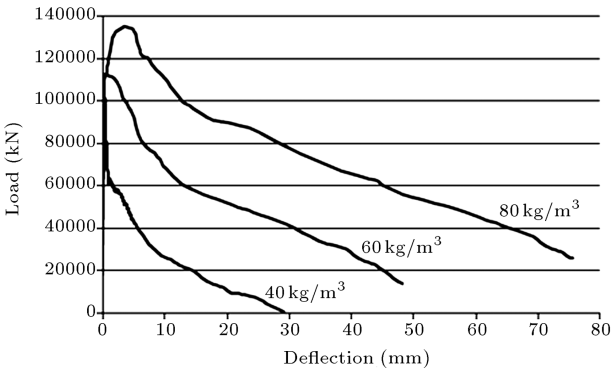

Figure 8. Load-deflection curve for steel fiber-reinforced slabs with different volumetric values of steel fiber.

in [6] has been compared to that obtained from FEM analysis in Figure 9, which demonstrates that the agreement is satisfactory. Secondly, to verify the FEM results for steel fiber-reinforced slabs with those obtained from experiment, the cracking and ultimate loads calculated from FEM analyses (with $k_s = 0$) for the slab with 60 kg/m^3 steel fibers were compared to experimental results. In actual fact, although the cracking and ultimate loads can be correctly obtained from FEM , the complete load-deflection curve after initial cracking cannot be extracted with FEM analysis, since the load gets decreased and the curve declines after cracking initiation. The mean cracking and ultimate loads obtained from the experiment were 71.6

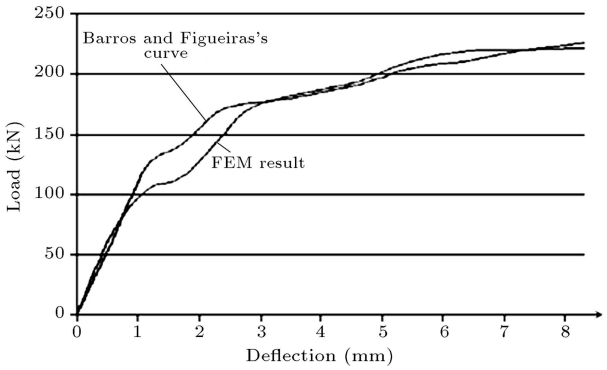

Figure 9. Comparison between the result of [6] and FEM results.

and 106 kN, respectively. Likewise, the values from FEM analysis were 73 and 108 kN, respectively. Thus, the concurrence between the results is satisfactory.

4.2. Spanning behavior of slabs

In order to distinguish the true spanning behavior of slab tracks, the distribution and magnitudes of positive and negative moments along and across the slab, and the positions of the beginning of cracks and their propagation pattern must be investigated. To this end, finite-element analysis was used. Based on the dimensions of experimental specimens, the length, width, and thickness of slabs were considered 2 m, 1.2 m, and 215 mm, respectively. The distance between fasteners was taken as 60 cm [17,18]. The Shell element with 6 degrees of freedom at each node was used to model the slabs, 3D beam elements were used to model the rails, and spring elements with nonlinear behavior were used for modeling the fasteners. The loads consisted of dead and live loads (considering the impact exerted by moving trains), lateral loads, and longitudinal forces caused by braking and acceleration of the train, all calculated or taken in accordance to UIC code [16]. To calculate the dead load, the volumetric mass of concrete was considered 2400 kg/m^3. The loads due to braking and acceleration of trains are equivalent to 1/7 the weight of the train. Also, the lateral load applied on the railway was computed as 38.3 kN [17].

Considering the impact influence, the most critical loading according to [19] is shown in Figure 10.

In the proposed models, the elasticity modulus and Poisson's ratio were taken 20 GPa and 0.17 for concrete, and 200 GPa and 0.3 for steel rails, respectively. Moreover, the stiffness of fasteners was considered 40 kN/mm, and the distance between them

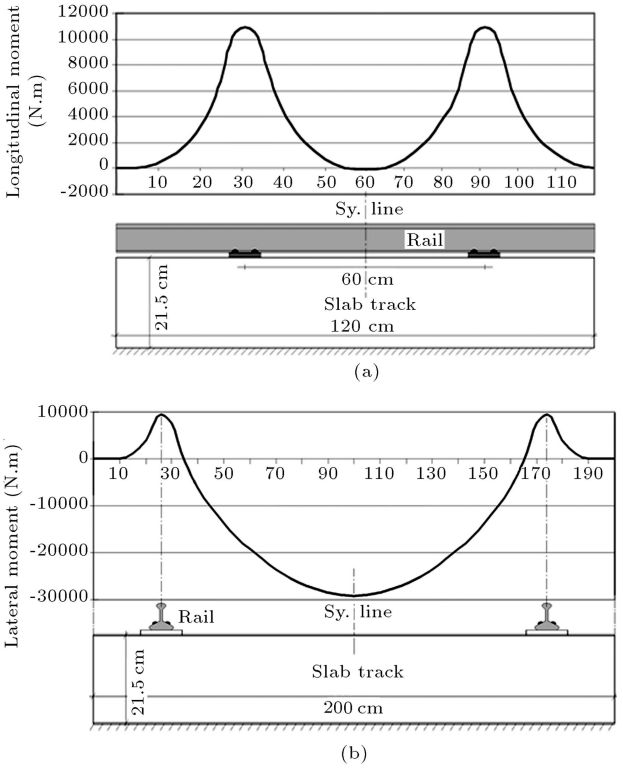

Figure 11. (a) Longitudinal and (b) lateral moment distribution of moments in a slab track with $k_s = 50$ MN/m^3 and 2 m width.

was taken 600 mm. Finally, the foundation modulus was taken 100 MN/m^3 [20].

The longitudinal and lateral distributions of moments for discrete slab systems with the foundation modulus of 50 MN/m^3 and 2 m width from FEM analyses are shown in Figure 11. This figure demonstrates that maximum moments and deflections occur under the concentrated wheel loads. Also, lateral moments are remarkably greater than longitudinal moments. Namely, the moment distribution is prevalent in the lateral direction, and thus, the flexural spanning behavior is one-way. Further analyses proved that the positions of maximum moments and deflections are not sensitive towards the foundation modulus. However, Figures 12 and 13 show that, by varying k_s, different effects on the positive and negative moments, either longitudinally or laterally, are observed. The positive moment always gets increased, due to increasing k_s, up to 150 MN/m^3. From this k_s onwards, the positive moment gets decreased. All the same, the negative moment invariably decreases with k_s. Compared to

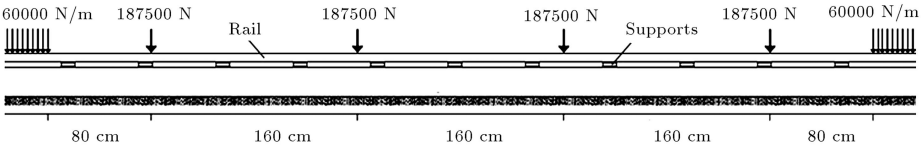

Figure 10. The loading scheme of the slab track system according to [20].

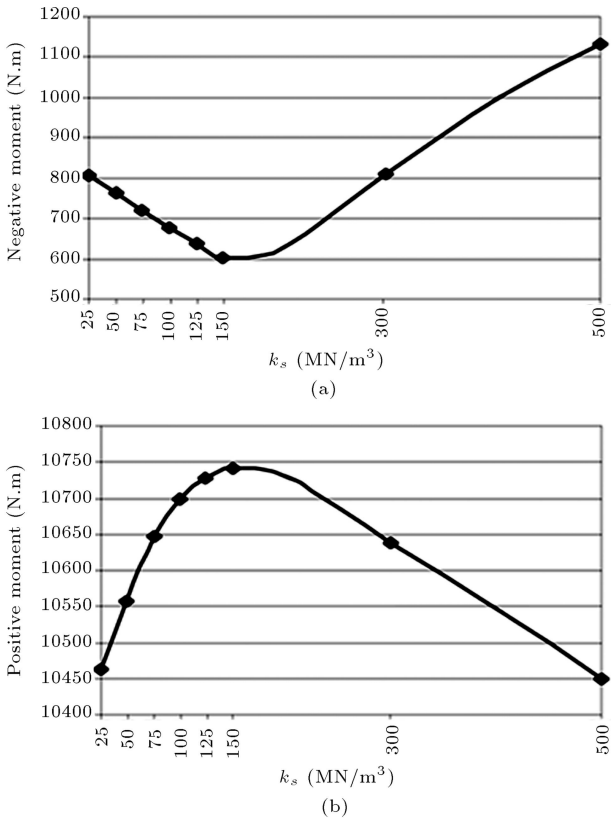

Figure 12. (a) Positive and (b) negative longitudinal moment variation with k_s.

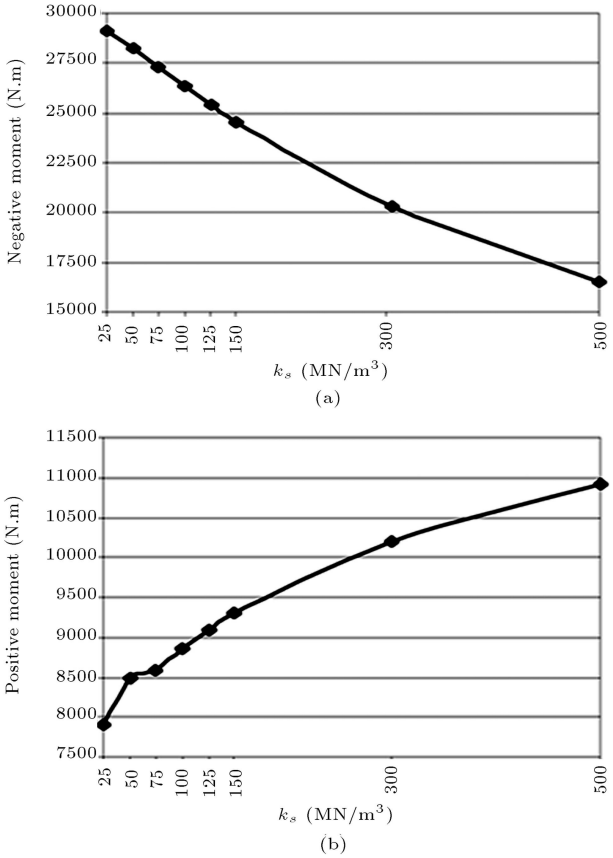

Figure 13. (a) Positive and (b) negative lateral moment variation with k_s.

continuous systems, the same results can be gathered, except that the deflection in continuous systems is slightly more than that in discrete systems. It can be inferred also from these figures that the lateral moments are greater than the longitudinal moments. Thus, the spanning behavior of slab tracks is one-way in both discrete and continuous systems.

4.3. Crack propagation

The stages of crack propagation for the continuous slab track systems are shown in Figure 14. The crack propagation pattern lends credibility to the one-way spanning behavior of slab tracks. The amount of k_s only causes the cracks to become less widely extended, but does not change the cracking pattern.

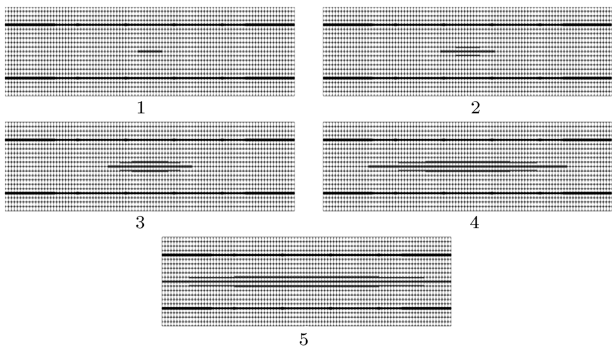

Figure 14. Stages of cracking in continuous slab track systems.

4.4. Critical and optimum widths

Table 2 shows the effect of varying width on the lateral moments of the slab track. This table reveals that the more the width, the less the negative moment and the more the positive moment will be. Since reducing the negative moment improves resistance against the loads, increasing the slab width is a promising way to have more safety in the structure [18]. Analyses indicated that when the width equals the distance between the rails (1.5 m), the positive moment vanishes. Moreover, the optimum width, for which the positive and negative moments are equal, is 2.5 m.

4.5. Load-deflection curves for slabs on foundation

The schematic outline of dimensions and loads corresponding to the effect of k_s are shown in Figure 15(a). The optimum slab width (2.5 m) was considered. $\varphi = 0$ signifies the contraflection (zero moment) point as shown in Figure 15(b). The deflection considered in the curves is the (average) difference between the deflection(s) of contraflection point(s) with that of the center point. Taking the steel fiber content to be 60 kg/m^3, the load-deflection curves for steel fiber-reinforced slabs are obtained as shown in Figure 16.

Table 2. Effect of slab width on the lateral moment.

k_s(MN/m^3)	Width (m)	Negative lateral moment (MN.m)	Psitive lateral moment (MN.m)
25	2.0	29149	7909
	2.5	13496	10153
	3.0	1824	21023
50	2.0	28281	8781
	2.5	13078	10481
	3.0	2912	20421
75	2.0	27312	8594
	2.5	12667	10682
	3.0	3767	19951
100	2.0	26354	8864
	2.5	12287	10855
	3.0	4421	19567

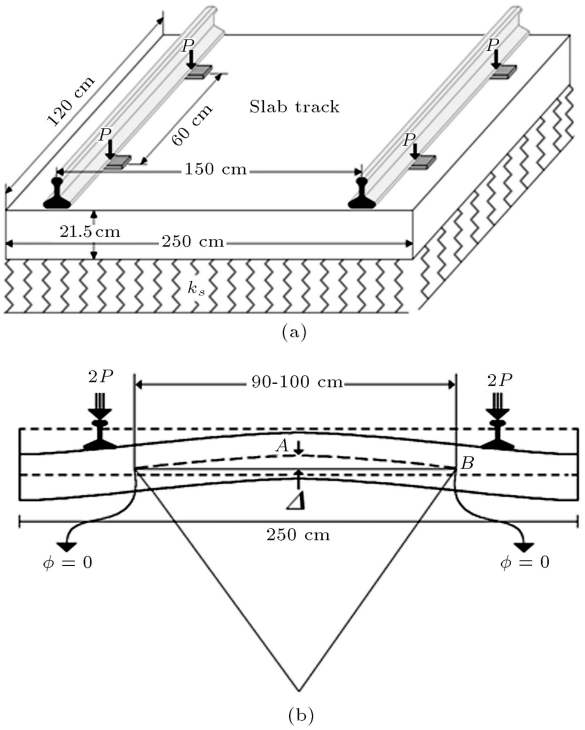

Figure 15. Effect of k_s on the load-deflection curve: (a) Model dimensions, and (b) deflection considered in the curves.

As observed in this figure, increasing k_s will cause both cracking and ultimate loads to increase, but decreases the energy absorption, i.e. the area beneath the load-deflection curve [12].

4.6. Effect of slab width on the fracture pattern

If three slab tracks have identical mechanical properties but one has a 2.5 m width, one has more-than-2.5 m width, and one has less-than-2.5 m width, the cracking behavior will differ in those slabs. In the slab with less-than-2.5 m width, cracking initiates from the middle of the upper face due to negative moments. In the slab with 2.5 m width, cracking initiates from the middle of the upper face, and immediately after that, continues in the lower face along the rails. Stated another way, cracking occurs firstly because of negative moments and immediately afterwards continue because of positive moments. Finally, in the slab with more-than-2.5 m width, cracking initiates from the lower face due to positive moments. Three instances of cracking in the three above-mentioned cases are shown in Figures 17-19.

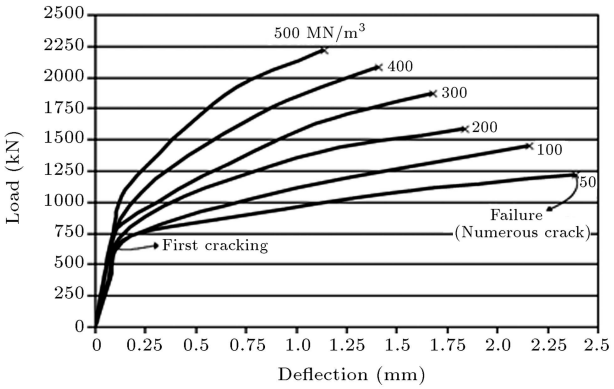

Figure 16. Effect of k_s on the load-deflection of steel fiber-reinforced slabs with 2.5 m width.

4.7. Effect of tensile strength and foundation modulus on the cracking and ultimate loads (design purposes)

Due to the fact that the bending test was exerted on prismatic specimens, the ultimate tensile stress, i.e. the tensile strength, can be directly calculated after initial cracking. The tensile strength calculated thus is more realistic, and the formulas proposed in some building codes overestimate this value. The tensile

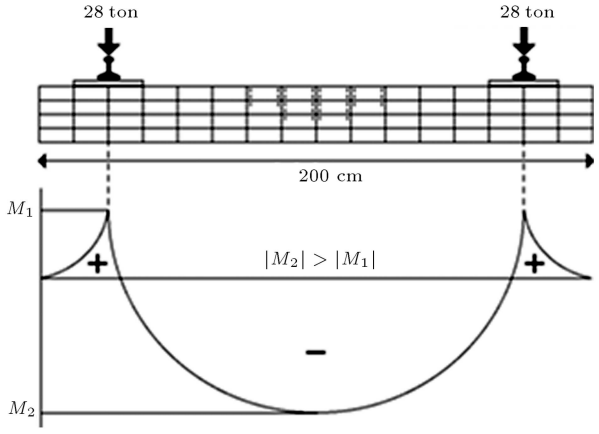

Figure 17. Cracking initiation in a slab with $b = 2$ m and $k_s = 300$ MN/m^3.

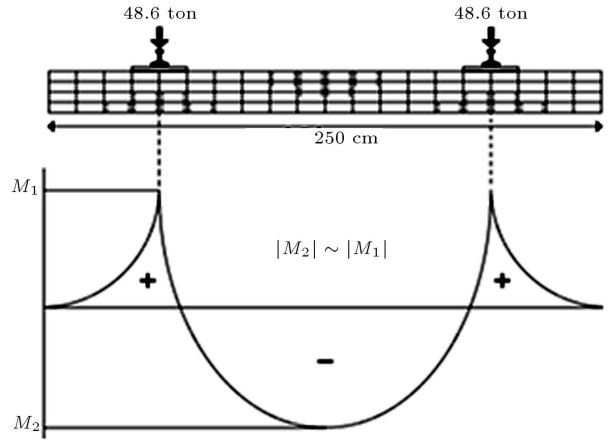

Figure 18. Cracking initiation in a slab with $b = 2.5$ m and $k_s = 300$ MN/m^3.

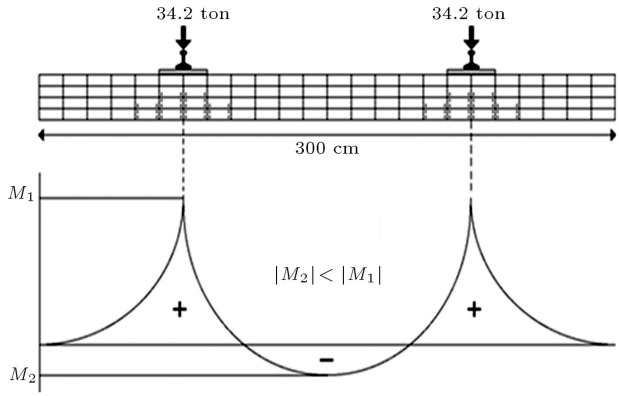

Figure 19. Cracking initiation in a slab with $b = 3$ m and $k_s = 300$ MN/m^3.

strength (σ_t) considered in previous analyses was 5.1 MPa, which corresponds to the tests with the mean amount of fiber content (60 kg/m^3). In order to account for other fiber content which leads to different tensile strengths, cracking loads with different values of k_s's and σ_t's are included in Tables 3 and 4 for 2.5 m width and 2 m width slabs, respectively. The same effect on the ultimate load capacity is presented in Tables 5 and 6. As can be obviously seen, the cracking and ultimate loads belonging to 2 m width slabs have remarkably lower values than those in slabs with optimum width.

Table 3. Cracking loads for slabs with 2.5 m width.

k_s	σ_t(MPa)						
(MN/m^3)	2.0	2.5	3.0	3.5	4.0	4.5	5.1
50	27.6	35.2	41.4	49.6	55.2	63.4	71.7
100	29.2	36.7	46.1	51.2	61.4	66.5	76.7
200	31.8	39.9	55.9	63.8	71.8	75.8	80.6
300	36.2	44.2	57.3	65.2	76.0	79.5	97.2
400	41.8	47.1	59.8	70.3	79.6	86.7	100.7
500	46.9	50.0	66.5	77.6	82.7	98.6	114.2

Table 4. Cracking loads for slabs with 2 m width.

k_s	$\sigma_t(MPa)$						
(MN/m^3)	2.0	2.5	3.0	3.5	4.0	4.5	5.1
50	21.6	26.2	31.4	37.1	42.2	47.4	52.6
100	22.2	27.5	33.1	39.2	43.7	48.9	54.7
200	25.1	29.9	36.9	41.8	47.8	53.2	59.2
300	26.2	30.5	38.3	44.2	49.0	54.5	61.2
400	27.8	34.1	42.8	47.3	54.6	61.7	68.2
500	29.9	38.0	45.5	51.6	58.7	66.2	73.2

Table 5. Ultimate loads for solid slabs with 2.5 m width.

k_s	$\sigma_t(MPa)$						
(MN/m^3)	2.0	2.5	3.0	3.5	4.0	4.5	5.1
50	47	62	72	83	96	108	120
100	58	71	86	101	115	130	144
200	63	82	96	112	128	144	160
300	74	95	111	130	150	167	186
400	83	105	124	145	166	185	207
500	88	112	133	155	177	199	221

Table 6. Ultimate loads for solid slabs with 2 m width.

k_s	$\sigma_t(MPa)$						
(MN/m^3)	2.0	2.5	3.0	3.5	4.0	4.5	5.1
50	44	54	66	76	88	99	110
100	53	68	81	93	108	121	135
200	61	78	92	107	124	140	155
300	65	80	98	113	130	147	159
400	70	86	102	117	135	151	163
500	74	90	107	122	139	156	171

For design purposes, the exerted loads must be factored. Using the load combination put forward in AASHTO [19], regarding the fact that dead loads are negligible, the factored load applied to the fasteners will be obtained as follows (D, L, and I stand for dead, live, and impact loads, respectively):

$$P_u = 3D + 2.17(L + I),$$

$$D \approx 0, L + I = 78.67\,\text{kN} \Rightarrow P_u \approx 171\,\text{kN}.$$

Each load is applied on a support as shown in Figure 20. Using this load applied, a slab track with a specific k_s and σ_t is analyzed by FEM and the maximum stress is compared with the rupture modulus. Thus, based on the above tables, the ranges of k_s for which the slab behaves safely can be plotted versus σ_t, as shown in Figure 21. This figure reveals that the slab with

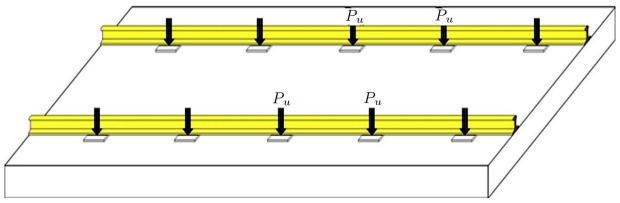

Figure 20. Factored loads applied on the slab track.

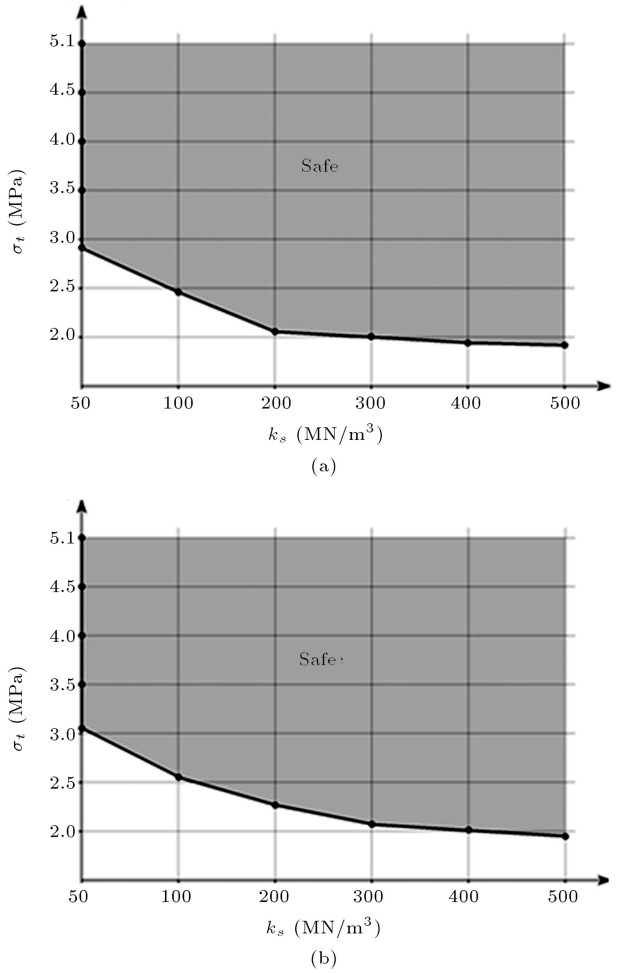

Figure 21. Permissible loading regions of slabs for (a) optimum-width (2.5 m), and (b) 2 m width slabs.

optimum width has a larger permissible region. Also, by increasing k_s, the required quality of concrete (σ_t) is lower, and conversely.

4.8. Comparison between the cracking and service moments and deflections

It would be interesting to make a comparison between the moment and deflection caused by service loads (before and after applying the 2.17 load factor) and the cracking moment in different geometric properties to conclude which case is more trustworthy. Table 7 shows the comparison between the moments and maximum deflections (in the middle of the slab track). In these analyses, k_s and σ_t have been taken as 50 MN/m^3 and 5.1 MPa, respectively. The experimental cracking moments in both 2 m and 2.5 m slab tracks were obtained 4 t.m, which demonstrate the good agreement between the results. This table reveals that, in the case of using the optimum-width (2.5 m) slab, the factored moment will be less than the cracking moment, while the factored moment is more than the cracking moment for widths other than 2.5 m, which propels the slab track into the nonlinear region. Thus, the optimum-width slab track is still more structurally reliable.

Table 7. Comparison between the service load moment and the cracking moment for different slab widths.

b=2m				
M_s (t.m)	M factored	M_c(t.m)	Δ_s (mm)	Δ_c (mm)
2.9	6.293	4.4	0.175	0.3
b = 2.5m				
M_s (t.m)	M factored	M_c (t.m)	Δ_s (mm)	Δ_c (mm)
1.7	3.689	4.4	0.045	0.13

5. Concluding remarks

Using non-ballast slab tracks with steel fibers is constructively efficient, accelerating and further facilitating construction, and mechanically efficient because of having considerable strength and more durability. In the present article, mechanical properties of steel fiber-reinforced slab tracks on nonlinear foundations were evaluated using FEM analysis. To this end, primary slab models were made to figure out the prevailing spanning direction and it was observed that slab tracks have one-way behavior. In the second stage, realistic models were made to study the effects of several parameters on the cracking and ultimate loads. The accuracy of models was assured by comparing the load-deflection curves with the corresponding curves obtained from previous experiments. It was deduced that the slab with 2.5 m width had the highest efficiency concerning the cracking and ultimate loads, the ratio of the moment under service loads to the cracking moment, and the safety region between the moment under factored loads and the cracking moment. Also, the cracking pattern changed at the 2.5 m width. The load-deflection curves revealed that, by increasing the foundation modulus or the concrete quality (the tensile strength), the cracking and ultimate loads, as well as energy absorption (the area beneath the curve), get increased. However, the settlements corresponding to the cracking threshold and the ultimate fracture get decreased. Finally, based on the obtained fracture loads, design curves were plotted to resist factored loads based on AASHTO.

Nomenclature

b	Slab width
D	Dead load
E_c	Concrete elasticity modulus
f'_c	Concrete compressive strength
I	Impact load
k_s	Foundation stiffness
L	Live load
P_u	Ultimate load
ε	Flexural strain
ε_0	Flexural strain corresponding to the maximum stress
Δ_u	Ultimate deflection
Δ_y	Yield-point deflection
φ	Curvature
M_s	Moment under service loads
M_c	Cracking moment
σ	Flexural stress
σ_t	Tensile strength

References

1. Esveld, C., *Slab Track: A Competitive Solution,* Faculty of Civil Engineering, Section of Roads and Railways, Delft University of Technology, the Netherlands (1999).
2. Esveld, C., *Recent Developments in Slab Track,* Faculty of Civil Engineering, Section of Roads and Railways, Delft University of Technology, the Netherlands, pp. 81-85 (2003).
3. Buyle Bodin, F. and Madhkhan, M. "Seismic behavior of steel fiber reinforced concrete piles", *Journal of Materials and Structures*, **35**, pp. 402-407 (2002).
4. Buyle Bodin, F. and Madhkhan, M. "Performance and modeling of seel fiber reinforced piles under seismic loading", *Journal of Engineering Structures,* **24**, pp. 1049-1056 (2002).
5. Madhkhan, M., Azizkhani, R. and Torki, M. E. "Roller compacted concrete pavements reinforced with steel and polypropylene fibers", *Journal of Structural Engineering and Mechanics* (Techno press), **40**(2), pp. 149-165 (2011).
6. Barros, J.A.O. and Figueiras, J.A. "Model for the Analysis of Steel Fiber Reinforced Concrete Slabs on Grade", *Journal of Computers and Structures*, **79**, pp. 97-106 (2001).
7. Falkner, H. and Teutsch, M. "Comparative investigations of plain and steel fiber-reinforced industrial ground slabs", Institut fur Baustoffe Massivbau und Brandschutz, Technical University of Brunswick, Germany, **102**, pp. 45-51 (1993).
8. Iran Railway Development Consultant Engineers, *Design of Different Non-ballasted Railway Systems*, Railway of Islamic Republic of Iran, Ministry of Routes and Transport, Tehran, Islamic Republic of Iran (2002).
9. Khaloo, A.R. and Afshari, M. "Flexural behavior of small steel fiber reinforced concrete slabs", *Journal of Cement and Concrete Composites*, **27**, pp. 141-149 (2005).
10. Smadi, M.M. and Bani Yasin, I.S. "Behavior of high-strength fibrous concrete slab-column connections under gravity and lateral loads", *Journal of Construction and Building Materials*, **22**, pp. 1863-1873 (2008).
11. Madhkhan, M., Entezam, M. and Torki, M.E. "Mechanical properties of precast reinforced concrete slab tracks on non-ballasted foundations", *Journal of Scientia Iranica, Trans. A.* **19**(1), pp. 20-26 (2012).
12. Timoshenko, S.P. and Gere, J.M., *Mechanics of Materials*, PWS Publishing Company, Boston, Massachusetts (1977).
13. Madhkhan, M. "Etude du comportment des dieux en beton de fibres metalliques sous solicitation sismique", These de Doctorat, Universite des Sciences et Technologies de Lille, Lille, France (1999).
14. Vellore, S., Gopalaratnam, V.S. and Gettu, R. "On the characterization of flexural toughness in fiber reinforced concrete", *Journal of Cement and Concrete Composites*, **17**, pp. 239-254 (1993).
15. ASTM C1018-97 "Standard test method for flexural youghness and first-crack strength of fiber reinforced concrete (using beam with third point loading)", 04.02 Standard Designation C1018-97, 8 p (2004).
16. UIC, *The Railways- An Indispensable Part of the European Transport System*, International Union of Railways, Paris France (1994).
17. Esveld, C., *Modern Railway Track*, MRT Productions, Zaltbommel, the Netherlands (2001).
18. Esveld, C., *Developments in High-Speed Track Design*, Faculty of Civil Engineering, Section of Roads and Railways, Delft University of Technology, the Netherlands (2004).
19. American Association of State Highway and Transportation Officials (AASHTO), *Standard Specifications for Highway Bridges*, 17th Ed. Washington, D.C., USA (2002).
20. Zwarthoed, J.M., Markine, V. and Esveld, C. "Slab track design: fexural stiffness versus soil improvement", in *Rail-Tech. Europe*, Utrecht, ISSN 0169-9288 CD-ROM, pp. 1-22, 3-5 April (2001).

Biographies

Morteza Madhkhan received his PhD degree from the University of Lille, France, and is currently Associate Professor in the Department of Civil Engineering at Isfahan University of Technology (IUT), Isfahan, Iran. His research interests include: advanced concrete technology, high strength concrete, and high performance concrete.

Alireza Entezam has a MS degree in Civil Engineering from Bou-Ali Sina University, Iran. His research interests include: experimental work on concrete technology.

Mohammad Ebrahim Torki Harchegani has a BS degree in Civil Engineering from Isfahan University of Technology (IUT), Iran, and a MS degree from Sharif University of Technology (SUT), Iran. His research interests include: experimental and analytical research in advanced concrete technology.